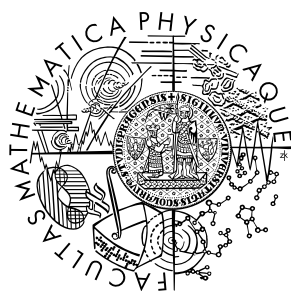


*A mesoscopical model of
shape-memory alloys*

Tomáš Roubíček & Martin Kružík & Jan Koutný

Preprint no. 2007-014



Research Team 1

Mathematical Institute of the Charles University

Sokolovská 83, 186 75 Praha 8

<http://ncmm.karlin.mff.cuni.cz/>

This is a preprint electronic version of the paper to be published in "Proc. Estonian Acad. Sci. Phys. Math."
The preprint and its maintaining in this preprint series is with permission of the Estonian Academy Publishers.

A mesoscopical model of shape-memory alloys¹

Tomáš ROUBÍČEK^{a,b}, Martin KRUŽÍK^{b,c}, Jan KOUTNÝ^b

^a Mathematical Institute, Charles University, Sokolovská 83, CZ-186 75 Praha 8, Czech Rep.

E-mail: tomas.roubicek@mff.cuni.cz

^b Institute of Information Theory and Automation, Academy of Sciences of the Czech Rep., Pod vodárenskou věží 4, CZ-182 08 Praha 8, Czech Republic.

E-mail: kruzik@utia.cas.cz, koutny@utia.cas.cz

^c Dept. of Physics, Faculty of Civil Engineering, Czech Technical University, Thákurova 7, CZ-16629 Praha 6, Czech Republic.

Abstract: Multiwell stored energy related to austenite and particular martensitic variants as well as a dissipation pseudopotential are used to assemble a mesoscopical model for an isothermal rate-independent martensitic transformation in shape-memory alloys. Theoretical results concerning numerical approximation of involved Young measures by laminates are surveyed and computational experiments are presented for CuAlNi single crystals.

Keywords: martensitic transformation, rate-independent processes, Young measures

1 Introduction, stored energy, microstructure, dissipation energy

Shape-memory alloys (=SMAs) belong to the so-called smart materials which enjoy important applications. SMAs exhibit specific, *hysteretic* stress/strain/temperature response and a so-called *shape-memory effect*. The mechanism behind it is quite simple: atoms tend to be arranged in several crystallographical configurations having different symmetry groups: higher symmetrical one (referred to as the *austenite* phase, typically cubic) has higher thermal capacity while lower symmetrical one (called the *martensite* phase, typically tetragonal, orthorhombic, or monoclinic) has lower thermal capacity and may exist, by symmetry, in several variants (typically 3, 6, or 12, respectively). We refer to [2, 4, 6, 14, 18, 20] for a thorough survey. Here we consider only isothermal stress/strain-response modeling.

We consider a bounded Lipschitz domain $\Omega \subset \mathbb{R}^3$ as a reference configuration (canonically the stress-free austenite). Standardly, the *displacement* $u : \Omega \rightarrow \mathbb{R}^3$ and the *deformation* $y : \Omega \rightarrow \mathbb{R}^3$ are related by $y(x) = x + u(x)$, $x \in \Omega$. Hence the *deformation gradient* is $F = \nabla y = \mathbb{I} + \nabla u$, where $\mathbb{I} \in \mathbb{R}^{3 \times 3}$ denotes the identity matrix. Mechanical response is phenomenologically described by a specific *stored energy* $\hat{\varphi} = \hat{\varphi}(F)$, assumed to have a p -polynomial growth/coercivity structure. The *frame-indifference*, i.e. $\hat{\varphi}(F) = \hat{\varphi}(RF)$ for any $R \in \text{SO}(3)$, the group of orientation-preserving rotations, requires that $\hat{\varphi}(\cdot)$ in fact depends only on the (right) Cauchy-Green stretch tensor $C := F^T F$. We abbreviate

$$\varphi(\cdot) := \hat{\varphi}(\mathbb{I} + \cdot). \quad (1.1)$$

¹ Supported by the grants 201/06/0352 (GA ČR), A 107 5402 (GA AV ČR), LC 06052, MSM 21620839 and VZ 6840770021 (MŠMT ČR), and MRTN-CT-2004-505226 (EU).

The overall free energy related to a displacement profile u is $\Phi(u) := \int_{\Omega} \varphi(\nabla u) dx$. Considering a (time-varying) elastic support $w(t, x)$ on a part Γ of the boundary $\partial\Omega$, we expand it to the stored energy $G(t, u) = \Phi(u) + \frac{1}{2} \int_{\Gamma} (u - w(t, \cdot))^{\top} B(u - w(t, \cdot)) dS$ with $B^{\top} = B$. Due to the multiwell character of φ , the deformation gradient usually tends to develop fast spatial oscillations if it tends to minimize the overall stored energy under given boundary conditions, see [1, 2, 14, 19], resulting to a *microstructure* that can effectively be described by so-called *gradient Young measures*, which are measurably parameterized probability measures $x \mapsto \nu_x$ on $\mathbb{R}^{3 \times 3}$ that can be attained by gradients in the sense $\lim_{k \rightarrow \infty} \int_{\Omega} g(x) \nu(\nabla u_k(x)) dx = \int_{\Omega} g(x) \int_{\mathbb{R}^{3 \times 3}} v(A) \nu_x(dA) dx$ for some sequence $\{u_k\}_{k \in \mathbb{N}} \subset W^{1,p}(\Omega; \mathbb{R}^3)$ and all $g \in L^{\infty}(\Omega)$ and $v \in C_0(\mathbb{R}^{3 \times 3})$, see [19]; the notation C_0 , L^p , $W^{1,p}$ for function spaces is standard. Let us denote the set of all such parameterized measures by $\mathcal{G}^p(\Omega; \mathbb{R}^{3 \times 3})$. The continuously extended (so-called *relaxed*) stored energy is then

$$\bar{G}(t, u, \nu) = \int_{\Omega} \int_{\mathbb{R}^{3 \times 3}} \varphi(A) \nu_x(dA) dx + \int_{\Gamma} \frac{(u - w(t, \cdot))^{\top} B(u - w(t, \cdot))}{2} dS. \quad (1.2)$$

The pair of “macroscopical” displacement u and the gradient Young measures ν represents a quite natural *mesoscopic description* of the state of the body. The “kinematically” admissible pairs (u, ν) are in

$$Q := \left\{ (u, \nu) \in W^{1,p}(\Omega; \mathbb{R}^3) \times \mathcal{G}^p(\Omega; \mathbb{R}^{3 \times 3}); \int_{\mathbb{R}^{3 \times 3}} A \nu_x(dA) = \nabla u(x) \text{ for a.a. } x \right\}.$$

Within microstructure evolution due to time-varying loading w , SMAs *dissipate energy*. For sufficiently slow loading, these processes are *activated* and quite *rate independent*, leading to a *hysteretic* stress/strain response. We assume dissipative forces having a (pseudo)potential, say R , and that the energy dissipated during the phase-transformation process depends (counting phenomenologically, beside possible rank-one connections, with various impurities) on the starting and the final (phase)variants, only; this (simplifying) concept has been adopted also in [5, 21, 25, 26, 27]. We implement this philosophy with help of a frame-invariant “phase indicator” being a smooth bounded function $\hat{\mathcal{L}} : \mathbb{R}^{3 \times 3} \rightarrow \mathbb{R}^L$ with L denoting number of (phase) variants. Then, with $\mathcal{L}(A) := \hat{\mathcal{L}}(\mathbb{I} + A)$ like (1.1), the dissipation potential is postulated as

$$R(\nu) := \int_{\Omega} \delta_K^*(\lambda(x)) dx \quad \text{with} \quad \lambda(x) = \int_{\mathbb{R}^{3 \times 3}} \mathcal{L}(A) \nu_x(dA) dx \quad (1.3)$$

with a convex compact $K \subset \mathbb{R}^L$ determining the *activation stresses*, δ_K being its indicator function, and δ_K^* its conjugate which is, of course, homogeneous degree-1. The quantity λ plays the role of a macroscopic *volume fraction* assigned through (1.3) to the microstructure described by ν .

2 Energetic solution, laminates, numerical approximation

Neglecting kinetic energy and based on *minimum-stored-energy principle* competing with *maximum-dissipation* (or rather *realizability* [9]) *principle*, in the scalar (hence convex) case, the desired evolution $(u, \nu) = (u(t), \nu(t)) : [0, T] \rightarrow Q$ would be governed by the doubly-nonlinear evolution inclusion

$$\begin{pmatrix} 0 & 0 \\ 0 & \partial R(\frac{d\nu}{dt}) \end{pmatrix} + \partial_{(u, \nu)} [\bar{G} + \delta Q](t, u, \nu) \ni 0 \quad \text{for } t \in [0, T], \quad (2.1)$$

considered completed by an initial condition, here on λ . In the convex case, it is equivalent (see [10, 12]) to the *energetic formulation*, i.e. *stability*

$$\forall(\tilde{u}, \tilde{\nu}) \in Q : \quad \bar{G}(t, u(t), \nu(t)) \leq \bar{G}(t, \tilde{u}, \tilde{\nu}) + R(\nu(t) - \tilde{\nu}). \quad (2.2)$$

together with the *energy equality*

$$\mathfrak{G}(t) + \text{Var}_R(\nu; s, t) = \mathfrak{G}(s) - \int_{(s,t) \times \Gamma} (u-w)^\top B \frac{\partial w}{\partial t} \, dS dt \quad (2.3)$$

to be satisfied for any $0 \leq s < t \leq T$, where $\mathfrak{G}(t) := \bar{G}(t, u(t), \nu(t))$ is the Gibbs energy and $\text{Var}_R(\nu; s, t)$ denotes the total variation over $[s, t]$ of $\nu(\cdot)$ with respect to R from (1.3). The particular terms in (2.3) represent the stored energy at time t , the energy dissipated by changes of the internal structure during the time interval $[s, t]$, the stored energy at the initial time s , and work done by external loadings during the time interval $[s, t]$. In our vectorial case, the set of admissible configurations Q is no longer convex hence (2.1) has no longer a good sense, and we must rely on the energetic formulation (2.2)–(2.3) as a natural generalization.

Mathematical advantage of the Mielke's -Theil's [10, 12, 13] energetic formulation (2.2)–(2.3) is that it is free of time derivatives. Existence of thus defined *energetic solution* $(u, \nu) : [0, T] \rightarrow Q$ has been showed in [11] provided \bar{G} is still regularized by counting energy of possible spatial jumps in λ , as proposed in [3, p.364].

For computational implementation, additional discretization of the set Q is necessary. Canonical approach is to apply P1-finite elements on a triangulation (with a discretization parameter h) of a polyhedral domain Ω for discretization u_h of u and element-wise constant (=homogeneous) so-called laminates (see [19]) to discretize ν . We implemented the *second-order laminate*, which leads to the four-atomic Young measure ν_h , where $\nu_h = \xi_{0h}\xi_{1h}\delta_{F_{1h}} + \xi_{0h}(1-\xi_{1h})\delta_{F_{2h}} + (1-\xi_{0h})\xi_{2h}\delta_{F_{3h}} + (1-\xi_{0h})(1-\xi_{2h})\delta_{F_{4h}}$ with $F_{1h} = \nabla u_h - (1-\xi_{0h})a_h \otimes n_h - (1-\xi_{1h})a_{1h} \otimes n_{1h}$, $F_{2h} = \nabla u_h - (1-\xi_{0h})a_h \otimes n_h + \xi_{1h}a_{1h} \otimes n_{1h}$, $F_{3h} = \nabla u_h + \xi_{0h}a_h \otimes n_h - (1-\xi_{2h})a_{2h} \otimes n_{2h}$, $F_{4h} = \nabla u_h + \xi_{0h}a_h \otimes n_h + \xi_{2h}a_{2h} \otimes n_{2h}$. Here $0 \leq \xi_{ih} \leq 1$, $i = 0, 1, 2$, are element-wise constant. The vectors $a_{ih} \in \mathbb{R}^3$ and $n_{ih} \in \mathbb{R}^3$ are element-wise constant as well and, moreover, we may choose $|n_{ih}| = 1$. Hence, the whole Young measure ν_h is identified by means of ∇u_h and $\{\xi_{ih}, a_{ih}, n_{ih}\}$. This ensures that $(u_h, \nu_h) \in Q$. The same approximation was used, for instance, in [8, 23].

In order to find an approximate energetic solution we consider a fully-implicit time discretization based on the following incremental problem: take a time step $\tau > 0$ and let ν_h^0 be a given initial condition (we do not prescribe an initial condition for u_h because R depends only on ν), and, for $k = 1, \dots, T/\tau \in \mathbb{N}$ we define recursively $(u_h^k, \nu_h^k)_{k=1, \dots, T/\tau}$ as a solution to the minimization problems

$$\left. \begin{array}{l} \text{Minimize} \quad \bar{G}(k\tau, u_h, \nu_h) + R(\nu_h - \nu_h^{k-1}) \\ \text{subject to} \quad (u_h, \nu_h) \in Q \text{ with} \\ \quad \quad \quad \nu_h \text{ element-wise constant 2nd-order laminates.} \end{array} \right\} \quad (2.4)$$

3 Computational experiments with CuAlNi

The *orthorhombic martensite* has 6 variants, i.e., counting also the austenite, $L = 7$. The frame-indifferent stored energy composed from St.Venant-Kirchhoff-type materials

for each (phase)variant is postulated as

$$\hat{\phi}(F) = \min_{\ell=0,\dots,6} \sum_{i,j,k,l=1}^3 \frac{\varepsilon_{ij}^\ell \mathcal{C}_{ijkl}^\ell \varepsilon_{kl}^\ell}{2} + d_\ell, \quad \varepsilon^\ell = \frac{R_\ell^\top (U_\ell^\top)^{-1} F^\top F U_\ell^{-1} R_\ell - \mathbb{I}}{2}, \quad (3.1)$$

where $\mathcal{C}^\ell = \{\mathcal{C}_{ijkl}^\ell\}$ is the 4th-order tensor of elastic moduli, R_ℓ rotation matrices related the martensitic coordinates to the reference austenite, d_ℓ some offsets, and U_ℓ the distortion matrices: $U_0 = \mathbb{I}$ corresponds to the austenite while

$$U_1 = \begin{pmatrix} \eta_2 & 0 & 0 \\ 0 & \eta_1 & \eta_3 \\ 0 & \eta_3 & \eta_1 \end{pmatrix}, \quad U_2 = \begin{pmatrix} \eta_1 & 0 & \eta_3 \\ 0 & \eta_2 & 0 \\ \eta_3 & 0 & \eta_1 \end{pmatrix}, \quad U_3 = \begin{pmatrix} \eta_1 & \eta_3 & 0 \\ \eta_3 & \eta_1 & 0 \\ 0 & 0 & \eta_2 \end{pmatrix} \quad (3.2)$$

while the other three, i.e. U_4, \dots, U_6 , take $-\eta_3$ in place of η_3 . An example of Cu-14.0wt%Al-4.2wt%Ni counts with $\eta_1 = 1.04245$, $\eta_2 = 0.9178$, and $\eta_3 = 0.01945$. The specific values of elastic moduli are determined from experiments; we refer to Sedláč et al. [24]. We also use the usual Voigt's notation which (in a one-to-one way) replaces \mathcal{C}^ℓ by $\{\mathcal{C}_{ij}^\ell\}_{i,j=1}^6$. For $\ell = 0$, i.e. for the austenite, by symmetry there are only 3 nonvanishing elastic moduli, i.e. here $\mathbb{C}_{11}^0 = \mathbb{C}_{22}^0 = \mathbb{C}_{33}^0 = 142.8$ GPa, $\mathbb{C}_{44}^0 = \mathbb{C}_{55}^0 = \mathbb{C}_{66}^0 = 93.5$ GPa, $\mathbb{C}_{12}^0 = \mathbb{C}_{23}^0 = \mathbb{C}_{13}^0 = 129.7$ GPa. The specific values for martensite (in the basis of a particular variant) are $\mathbb{C}_{11} = 189$ GPa, $\mathbb{C}_{22} = 141$ GPa, $\mathbb{C}_{33} = 205$ GPa, $\mathbb{C}_{44} = 54.9$ GPa, $\mathbb{C}_{55} = 19.7$ GPa, $\mathbb{C}_{66} = 62.6$ GPa, $\mathbb{C}_{12} = 124$ GPa, $\mathbb{C}_{13} = 45.5$ GPa, $\mathbb{C}_{23} = 115$ GPa. Matrices R_ℓ from (3.1) are proper rotations transforming \mathbb{C} to the basis of the austenite and can be found in [8]. The offset d_ℓ in (3.1) has been chosen as 3 MPa, which corresponds to the process temperature 312 K.

As to the construction of the phase-indicator function $\mathcal{L} : \mathbb{R}^{3 \times 3} \rightarrow \mathbb{R}^7$ we take some $\delta > 0$ small and a smooth function $d : \mathbb{R} \rightarrow \mathbb{R}$ such that $d = 1$ in a neighborhood of 0 and $d = \delta$ far from that neighborhood, and put

$$\hat{\mathcal{L}}(F) := \left\{ \frac{d(|F^\top F - U_\ell^\top U_\ell|_{\mathbb{F}}^2)}{\sum_{\ell=0}^6 d(|F^\top F - U_\ell^\top U_\ell|_{\mathbb{F}}^2)} \right\}_{\ell=0}^6. \quad (3.3)$$

The set K in (1.3) is chosen as a simplex in \mathbb{R}^7 and specific dissipation energies (or, equally, activation stresses) are set to be 2 MJ/m³ (=2 MPa) for transformations between austenite and martensite and 1 Pa for transformations between various variants of martensite, which makes the so-called re-orientation of martensite almost non-dissipative. It is an unfortunate reality that the data for the phenomenological dissipation model are very difficult to obtain. Moreover, dissipation mechanisms are often not fully autonomous and, e.g., may vary within number of cycles in cyclical loadings. Here, the concrete value 2 MJ/m³ is approximately fitted with experiments reported in [16, Fig.1] or [17, Fig.4] while the value 1 Pa is to reflect that the reorientation of two martensite variants which are rank-one connected is nearly nondissipative at least if there are not much impurities in the material so that pinning effects are small, cf. also [7] for the case of austenite/martensite transformation.

4 Results on compression tests

Our specimen is a block with dimensions 4×9×4 mm, referring to the stress-free austenite Ω . Its bottom is fixed by the zero-displacement Dirichlet boundary condition while on its

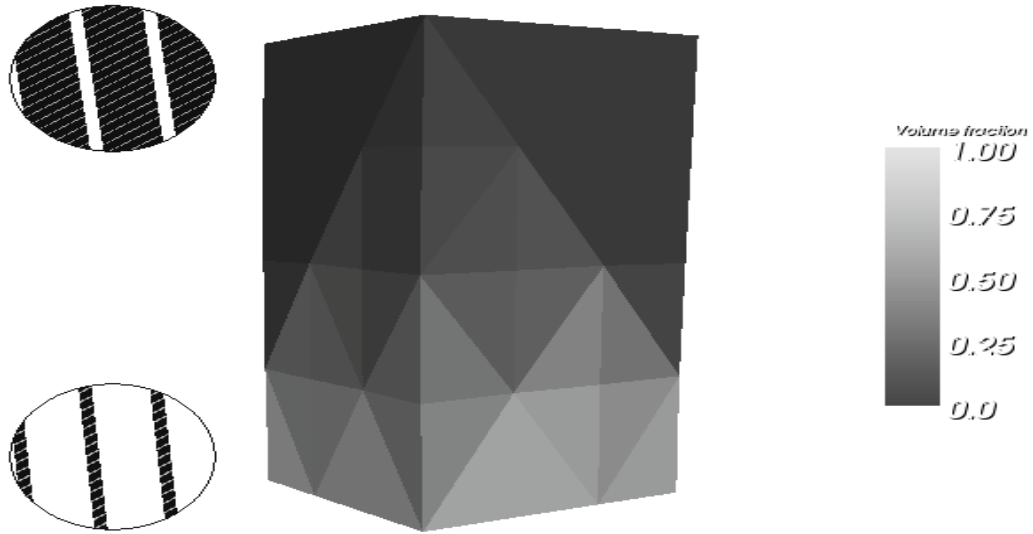


Figure 1: Specimen, here $(0, \text{tg}10^\circ, 1)$ -oriented CuAlNi single crystal, under compression loading at 200 MPa transforms from the austenite (gray) to a twinned martensite (black) composed from two variants, namely U_1 and U_2 , cf. (3.2). The austenite/twinned-martensite configuration reconstructed from computed Young measures is depicted on two chosen elements.

top we apply varying stress ranging the interval $0 - 300$ MPa in the vertical direction; cf. Figure 4. This may correspond to $w(t, \cdot) = 0$ and B a large positive multiple of the identity on the bottom and $B \rightarrow 0_+$ and $w(t, \cdot) \rightarrow \infty$ on the top of the specimen in the formula (1.2). The initial condition is $\nu_h^0 = \delta_0$, i.e., the whole specimen is in the austenite. The form of stored energy (3.1) together with variants (3.2) reflect the case when the crystal lattice of austenite has the orientation (001). In many applications, however, the specimen is oriented differently, see e.g. [15]. Various material orientations can be easily implemented by using the specific stored energy $\bar{\phi}(F) = \hat{\phi}(FR_A)$, where R_A is a rotation of the austenite from (001). Four compression tests were performed for $(0, \text{tg}\alpha, 1)$ -oriented single-crystal with $\alpha = 10, 20$, and 30 degrees, cf. Figure 4

It should be remarked that, in real CuAlNi single crystals, the 2H (γ'_1) orthorhombic martensite considered in the above text occurs in compression tests near the (001) directions while in directions closer to (011) or (111) another type of martensite, namely 18R (β'_1) which is monoclinic, may be observed, too. To model it, other 12 wells would have to be included into the stored energy as well as other dissipation energies would have to be specified. Beside such expansion of the energies in the model, the simulations would expectedly be more difficult because the optimization algorithms are computational less efficient if the landscape of the minimized energy in (2.4) has more local vales. In the compression test presented here, the monoclinic martensite seems indeed relatively negligible, as documented on [17, Fig.5], and therefore we dared neglect it. Also, our focus has been rather to present the modelling aspects and the ability of the model itself.

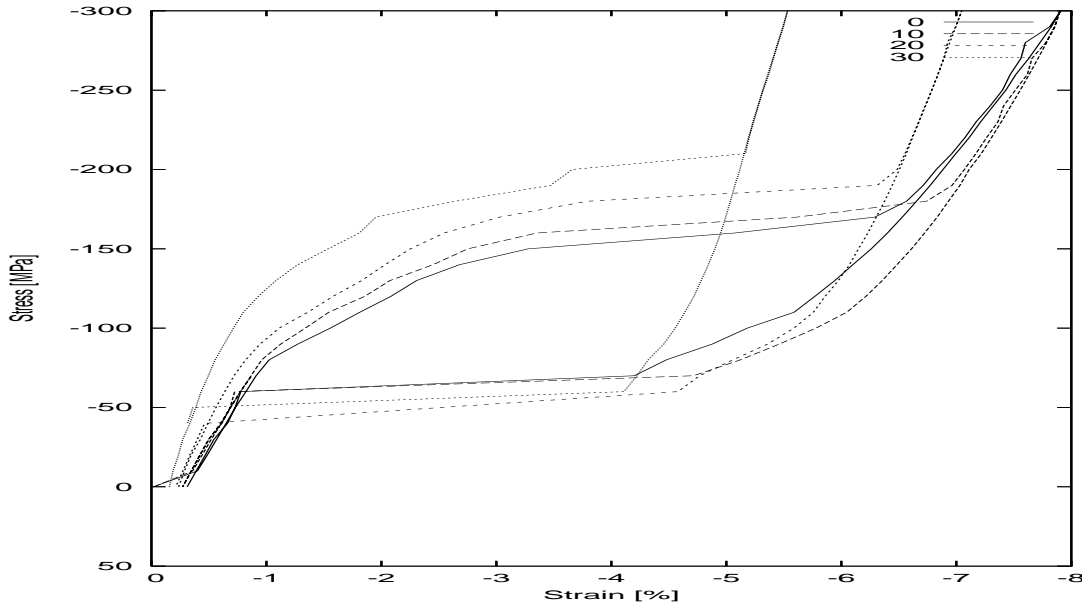


Figure 2: Stress-strain response under cyclic compression load of a $(0, \tan \alpha, 1)$ -oriented single-crystal depends substantially on α . Here $\alpha = 0^\circ, 10^\circ, 20^\circ$, and 30° is depicted.

References

- [1] Ball, J.M., James, R.D.: Fine phase mixtures as minimizers of energy. *Archive Rat. Mech. Anal.* **100** (1988), 13–52.
- [2] Bhattacharya, K.: *Microstructure of martensite. Why it forms and how it gives rise to the shape-memory effect*. Oxford Univ. Press, New York, 2003.
- [3] Frémond, M.: *Non-Smooth Thermomechanics*. Springer, Berlin, 2002.
- [4] Frémond, M., Miyazaki, S.: *Shape memory alloys*. Springer, Wien, 1996.
- [5] Huo, Y., Müller, I.: Nonequilibrium thermodynamics of pseudoelasticity. *Continuum Mech. Thermodyn.* **5** (1993), 163–204.
- [6] James, R.D., Hane, K.F.: Martensitic transformations and shape-memory materials. *Acta Mater.* **48** (2000), 197–222.
- [7] James, R.D., Zhang, Z.: A way to search for multiferroic materials with “unlikely” combination of physical properties. Chap.9 in: *Magnetism and Structure in Functional Materials*. (A.Planes, L.Manoza, A.Saxena, eds.), Springer, 2005, pp.159–176.
- [8] Kružík, M., Mielke, A., Roubíček, T., Modelling of microstructure and its evolution in SMA single-crystals, in particular in CuAlNi. *Meccanica* **40** (2005), 389–418.
- [9] Levitas, V.I.: The postulate of realizability. *Int. J. Eng. Sci.* **33** (1995), 921–971.
- [10] Mielke, A.: Evolution of rate-independent systems. In: *Handbook of Differential Equations*: (Eds. C.Dafermos, E.Feireisl), pp.461–559, Elsevier, Amsterdam, 2005.
- [11] Mielke, A., Roubíček, T.: Rate-independent model of inelastic behaviour of shape-memory alloys. *Multiscale Modeling Simul.* **1** (2003), 571–597.
- [12] Mielke, A., Theil, F.: On rate-independent hysteresis models. (accepted July 2001 for) *Nonlin. Diff. Eq. Appl.* **11** (2004) 151–189.

- [13] Mielke, A., Theil, F., Levitas, V.I.: A variational formulation of rate-independent phase transform. using an extremum principle. *Arch.Rat.Mech.Anal.* **162** (2002), 137–177.
- [14] Müller, S.: Variational models for microstructure and phase transitions. (Eds.: S.Hildebrandt et al.) *Lect. Notes in Math.* **1713** (1999), Springer, Berlin, pp.85–210.
- [15] Novak, V., Šittner, P., Ignacová, S., Černocho, T.: Transformation behavior of prism shaped shape memory alloy single crystals. *Icomat2005, Shanghai, China, Mat. Sci. Eng A* (2006), 755–762
- [16] Novak, V., Šittner, P., Zárubová, N.: Anisotropy of transformation characteristics of Cu-base alloys. *Material Science and Engr.* **A 234–236** (1997), 414–417.
- [17] Novak, V., Šittner, P., Vokoun, D., Zárubová, N.: On the anisotropy of martensitic transformation in Cu-based alloys. *Material Sci. and Engr.* **A 273–275** (1999), 280–285.
- [18] Otsuka, K., Shimizu, K.: Morphology and crystallography of thermoelastic Cu-Al-Ni martensite analyzed by the phenomenological theory. *Trans. Japan Inst. Metals* **15** (1974), 103–113.
- [19] Pedregal, P.: *Parametrized Measures and Variational Principles*. Birkhäuser, Basel, 1997.
- [20] Pitteri, M., Zanzotto, G.: *Continuum Models for Phase Transitions and Twinning in Crystals*. Chapman & Hall, Boca Raton, 2003.
- [21] Petryk, H.: Thermodynamic conditions for stability in materials with rate-independent dissipation. *Phil. Trans. Roy. Soc.* **A 363** (2005). 2479–2515.
- [22] Roubíček, T.: Models of microstructure evolution in shape memory materials. In: *Nonlin. Homogen. and its Appl.to Composites, Polycryst. and Smart Mater.* (Eds. P.Ponte Castaneda et al.), *NATO Sci.Ser.II/170*, Kluwer, Dordrecht, 2004, pp.269–304.
- [23] Roubíček, T., Kružík, M.: Mesoscopic model of microstructure evolution in shape memory alloys, its numerical analysis and computer implementation. *GAMM Mitteilungen*, **29** (2006), 192–214.
- [24] Sedlák, P., Seiner, H., Landa, M., Novák, V., Šittner, P., Mañosa, Ll.: Elastic constants of bcc austenite and 2H orthorhombic martensite in CuAlNi shape memory alloy. *Acta Mater.* **53** (2005), 3643–3661.
- [25] Stupkiewicz, S., Petryk, H.: Modelling of laminated microstructures in stress-induced martensitic transformations. *J. Mech. Phys. Solids* **50** (2002), 2303–2331.
- [26] Thamburaja, P., Anand, L.: Polycrystalline shape-memory materials: effect of crystallographic texture. *J. Mech. Physics Solids* **49** (2001), 709–737.
- [27] Vivet, A., Lexcelent, C.: Micromechanical modelling for tension-compression pseudoelastic behaviour of AuCd single crystals. *Euro Phys.J. A.P.* **4** (1998), 125–132.